

Fatigue Behaviour of New Eco-7175 Extruded Aluminium Alloy

Chinh Vu^a; Chien Wern^b; Bong-Hwan Kim^c; Shae Kwang Kim^d; Ho-Joon Choi^e, Sung Yi^f

a Ph.D. Student, Portland State University, Portland, OR, United States. E-mail: cvu@pdx.edu

b Associate Professor, Portland State University, Portland, OR, United States. E-mail: wernc@pdx.edu

c Principal Researcher, Korea Institute of Industrial Technology, 7-47 Songdo-dong, Incheon 406-840, Korea. E-mail: bonghk75@kitech.re.kr

d Principal Researcher, Korea Institute of Industrial Technology, 7-47 Songdo-dong, Incheon 406-840, Korea. E-mail: shae@kitech.re.kr

e Director, Korea Institute of Industrial Technology, 7-47 Songdo-dong, Incheon 406-840, Korea. E-mail: hjoon@kitech.re.kr

f Professor, Portland State University, Portland, OR, United States. E-mail: syi@pdx.edu

Abstract

Fatigue characteristics of a new extruded aluminium 7175, with an experimental composition where a magnesium-calcium alloy is used during the alloying process instead of the standard pure magnesium, is investigated. This new aluminium 7175, dubbed as aluminium ECO7175v1, results in a cleaner manufacturing process and improves mechanical properties. The fatigue behavior of the new aluminium ECO7175v1 with T74 temper is investigated. Experimental data showed the fatigue life of ECO7175v1-T74 aluminium can exceed 10^7 cycles with a fatigue strength of approximately 207 MPa, about 36% of its tensile strength. Fractography results show that failure modes are predominately ductile near the surface while brittle towards the center. In addition, at higher stresses, there are typically more crack initiation points at or near the surface of the specimens compared to specimens at lower stresses. Irrespective of the stresses the specimens are subjected to, all crack initiation points are located near or at the surface and no inclusions to act as stress concentrators are seen.

1. Introduction

Aluminium is an abundant material that is relatively soft, ductile, malleable, and lightweight. Aluminium also has good strength-to-weight ratio, high corrosion resistance, and low thermal expansion. As a result, it is widely used in the aerospace industry due to many of its attractive properties. However, the inherent strength of the material leaves more to be desired. Therefore, aluminium is typically alloyed with other elements to improve its strength. The increased strength is particularly important when taking fatigue resistance into consideration. Materials with higher strengths have higher fatigue resistances.

To improve upon its strength and other properties, aluminium is commonly alloyed with various elements such as copper and zinc. Aluminium alloys are available in series where the standard naming scheme is designed by the International Alloy Designation System [1]. It is given a four-digit number where the first digit indicates the major alloying element, the third and fourth digits are for identification of the specific alloy composition in the series, and the second digit, if it's not 0, indicates the variation of the alloy identified in the third and fourth digits. Aluminium 2000 series has copper as the primary alloying element, manganese for the 3000 series, silicon for the 4000 series, magnesium for the 5000 series, zinc for the 7000 series, and combinations of elements such as magnesium and silicon for the 6000 series. Finally, for all else not under the standard 2000 to 7000 series, is named and placed under the 8000 series.

Aluminium 7175 is from the 7000 series in which zinc is the primary alloying element granting it excellent combinations of strength and toughness, thus, has the highest strength of any aluminium alloy [3]. Aluminium 7000 series, as a result, is often used in the aircraft industry and is slowly superseding the 2000 series. In addition, aluminium 7000 series can be further strengthened through precipitation hardening. Aluminium 7175 is a variant of

the standard 7075 with the same composition but has fewer impurities, therefore, giving 7175 superior properties in strength and toughness [9].

In the present study, a variant of the standard 7175 aluminium alloy, named as ECO7175v1, was designed and fabricated. The “ECO” in the variant name indicates that the material is more economical and environmentally friendly than the standard 7175 aluminium alloy series. The primary concept behind the new ECO aluminium alloys is the usage of Eco-Mg, a magnesium-calcium alloy, instead of pure magnesium as the alloying element [5].

Magnesium is one of the primary alloying elements beside zinc in the aluminium 7000 series. Magnesium is used as an alloying element as it significantly increases the strength of the alloy as well as the alloy’s resistance to corrosion. However, magnesium is highly reactive and oxidative at high temperatures, resulting in significant loss of magnesium through slag during the manufacturing process [12]. To reduce this loss, protective gases such as sulfur hexafluoride (SF6) and fluxes are used. These protective gases are expensive and not environmentally friendly as sulfur hexafluoride is an extremely potent greenhouse gas. By alloying magnesium with calcium, the resulting magnesium alloy has significantly higher oxidation resistance at high temperatures and requires less protective gases [7]. The new magnesium-calcium alloy is subsequently added to aluminium to produce a modified 7175 aluminium alloy with improved mechanical properties as a side-effect of the cleaner manufacturing process [6]. The mechanical properties are improved because the cleanliness of the process resulted in clean molten aluminium with greatly reduced oxides and inclusions through controlled oxidation of the magnesium during the melting, holding, transferring, pouring, and filling [5]. The lack of, or reduced usage, of expensive protective gases and the improved efficiency of the manufacturing process reduced the overall cost of production.

Table 1: Manufactured Composition of Aluminum ECO7175v1-T74.

| Element | Composition % |
|----------------|---------------|
| Aluminum (Al) | Balance |
| Calcium (Ca) | 0.041 |
| Chromium (Cr) | 0.21 |
| Copper (Cu) | 1.74 |
| Iron (Fe) | 0.08 |
| Magnesium (Mg) | 2.73 |
| Manganese (Mn) | 0.01 |
| Silicon (Si) | 0.04 |
| Titanium (Ti) | 0.028 |
| Zinc (Zn) | 5.95 |

Generally, silicon and iron are not desired in aluminium alloys as they decrease the fatigue strength of the material through the formation of Al_7Cu_2Fe and Mg_2Si [8]. However, silicon and iron are present in the specimens because they are impurities which are typically found in stock aluminium. They are expected in aluminium alloys with a maximum allowable composition of 0.15% for silicon and 0.20% for iron. The use of magnesium-calcium alloy also has the added benefit of reducing the formation of Mg_2Si through controlled oxidation, resulting in improved fatigue strength. The composition of ECO7175v1-T74 is given in Table 1.

The tensile strength of ECO7175v1-T74 was determined through tensile tests and is tabulated in Table 2 where it is compared with several other variants of aluminium 7175. Aerospace Material Specification (AMS) 4149 and AMS 4344 are fabrication specifications for aluminium 7175 alloy. AMS 4149 aluminium is manufactured through forging (die forging or hand forging) and subjected to T74 temper. AMS 4344 aluminium is manufactured through extrusion and subjected to T73511 temper. T74 temper indicates the alloy is tempered with the base T7 temper where the alloy is solution heat treated, quenched, and then overaged in a furnace. Further treatment, indicated by the second digit “4” in “74,” is used to further enhance the strength, toughness, fracture toughness, and corrosion resistance [4]. T73511 temper is a variation of the T73 temper where the base temper is T7 with further treatment to increase stress-corrosion resistance of the alloy.

Fatigue is a major failure mechanism in aerospace structures, thus, plays an important role in determining the reliability of an aircraft. Fatigue failure occurs under repeated applied stresses which cause localized progressive structural damage to the material even though the applied stress is significantly less than the tensile strength of the material. In aerospace applications, various components are frequently subjected to these repeated stresses at high

frequencies. Therefore, it is imperative to know how many cycles these components can survive given the known repeated applied stresses. The fatigue behaviour of materials is described by an S-N curves where S is the stress amplitude of the cyclical stress, and N is cycles-to-failure. The particularly relevant feature of this curve is the endurance limit as it is assumed stresses below the endurance limit will not produce fatigue failure irrespective of how many cycles are applied (i.e. there is infinite life). In the simplest design cases, there is a need to keep all stresses below the endurance limit. However, it is widely accepted aluminium does not exhibit an endurance limit; instead, aluminium has a fatigue strength at a defined cycles-to-failure. Therefore, it is important to know the amplitude that causes failure up to 10^7 cycles.

Table 2: Tensile Properties of Aluminium 7175.

| Variant | TYS (MPa) | UTS (MPa) | EL. (%) | Reference |
|---------------|--------------|-------------|-----------|--|
| AMS 4149 | 441 | 510 | 7 | MMPDS-11, 7175-T74 (die forging) [2] |
| AMS 4149 | 434 | 503 | 9 | MMPDS-11, 7175-T74 (hand forging) [2] |
| AMS 4344 | 407 | 476 | - | MMPDS-11, 7175-T73511 (extrusion) [2] |
| ECO7175v1-T74 | 489.53±13.58 | 573.99±5.17 | 10.5±0.47 | Extrusion, T74 |

In this study, the new aluminium ECO7175v1-T74 is subjected to fatigue testing and fracture analysis. The results of the fatigue testing and fracture analysis were examined. Even though tensile behaviours of aluminium ECO7175v1-T74 are measured and known, little is known about the fatigue behaviours of this new material. Moreover, comparisons cannot be made since there are no available or comparable fatigue data for extruded aluminium 7175 with this composition with which to draw a comparison. Therefore, the primary purpose of this study is to measure fatigue strength for this new material and investigate its fracture characteristics.

2. Experimental Setup

In this study, the stress-life approach is employed to determine the strength of materials under the action of fatigue loads. The specimens are in an hourglass-shape with the dimensions shown in Figure 1. The specimens are subjected to cyclic bending loads. In determining fatigue stress levels using standard test equipment, the test specimens were subjected to a fully-reversed constant stress amplitude with stress ratio $R = -1$ where the cyclic stress varies from tensile to compressive with equal magnitude.

The fatigue testing machine used, as shown in Figure 2, model RFB200, is manufactured by Fatigue Dynamics, Inc.. The motor speed in RPM were measured and verified using a NIST Traceable OMEGA HHT13 non-contact laser tachometer with a factory tested certified accuracy of $\pm 0.01\%$ of reading. The setting for bending moment loads were calibrated and verified using a Vishay Micro-Measurements Rosette strain gauge coupled to a Vishay Precision Group's Model P3 Strain Indicator and Recorder.

Fatigue tests were conducted with a number of specimens per load while runouts are defined as over 10^7 cycles, as defined by the fatigue test conducted for aluminium AMS 4149 (7174-T74) in MMPDS-11 [2] Generally, the scatter in cycles-to-failure increases with decreasing bending moment loads. As the numbers of specimens is limited, they had to be allocated, as shown in Table 3, to maintain the desired 5% or less coefficient of variance with a confidence of 90% [10].

The fracture surface of broken specimens were then analysed using a Leica Microsystems' S6D StereoZoom optical microscope with a 0.75x objective lens coupled to an AmScope MU900 9-megapixel digital camera through a Leica Microsystems' 1.0x optical phototube. Further analysis of the surface of broken specimens were then analysed using a Zeiss Sigma VP FEG scanning electron microscope (SEM).

Table 3: Allocation of Specimens.

| Stress Amplitude (MPa) | Number of Specimens |
|------------------------|---------------------|
| 510 (89% UTS) | 10 |
| 448 (78% UTS) | 10 |

| | |
|---------------|----|
| 434 (76% UTS) | 10 |
| 393 (68% UTS) | 10 |
| 331 (58% UTS) | 13 |
| 262 (46% UTS) | 10 |
| 200 (35% UTS) | 5 |
| 138 (24% UTS) | 3 |

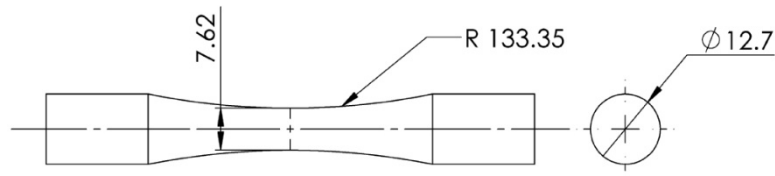


Figure 1: Fatigue coupon dimensions. Units are in millimeters.



Figure 2: Model RFB200 fatigue tester by Fatigue Dynamics. (Image by authors.)

3. Results and Discussions

The experimental fatigue test results are tabulated in Table 4. Fatigue test results for stress amplitude of 510 MPa, 448 MPa, and 331 MPa have a coefficient of variance of more than the desired 5%. Due to a limited number of specimens, it was decided to allocate more experimental specimens towards these stress amplitudes to bring coefficient of variance closer to 5%. After the allocation, the coefficient of variance for specimens loaded at 510 and 331 MPa are still considerably higher than 5% but are now considerably lower than previously.

Table 4: Statistical Analysis of Fatigue Testing.

| Stress Amplitude (MPa) | Average Log Cycles | Standard Deviation | Coefficient of Variance % |
|------------------------|--------------------|--------------------|---------------------------|
| 510 (89% UTS) | 3.581 | 0.216 | 6.0 |
| 448 (78% UTS) | 3.856 | 0.210 | 5.4 |
| 393 (68% UTS) | 4.159 | 0.180 | 4.3 |
| 331 (58% UTS) | 4.641 | 0.362 | 7.8 |
| 262 (46% UTS) | 5.041 | 0.158 | 3.1 |

| | |
|---------------|-------------------------------|
| 200 (35% UTS) | Run-outs (Over 10^7 Cycles) |
| 138 (24% UTS) | Run-outs (Over 10^7 Cycles) |

Figure 3 shows the S-N curve for ECO7175v1-T74 fatigue test. The S-N curve covers from a range of 10^3 cycles all the way to 10^7 cycles. The majority of the cycles-to-failure above 207 MPa are between 10^3 and 10^6 cycles. 207 MPa, approximately 36% of its tensile strength of 574 MPa, is also approximately the fatigue strength of the material at 10^7 cycles.

There is no other data that can be compared directly with the fatigue test results of the new ECO7175v1-T74 alloy. The closest data to compare would be of AMS 4149 (7175-T74) which is un-notched, hand forged, longitudinal, and transverse direction, as given by the MMPDS-11 handbook. However, there are many differences in the specimen geometry, fabrication process, and the testing method. ECO7175v1-T74's minor diameter is 0.30 inch compared to AMS 4149 0.25 inch. AMS 4149 was forged instead of extruded. ECO7175v1-T74 was subjected to fully-reversed bending loads with a stress ratio $R = -1$ rather than an axial load with a stress ratio R of 0.10 and 0.50, as in the case for AMS 4149. All these differences make comparison results not viable.

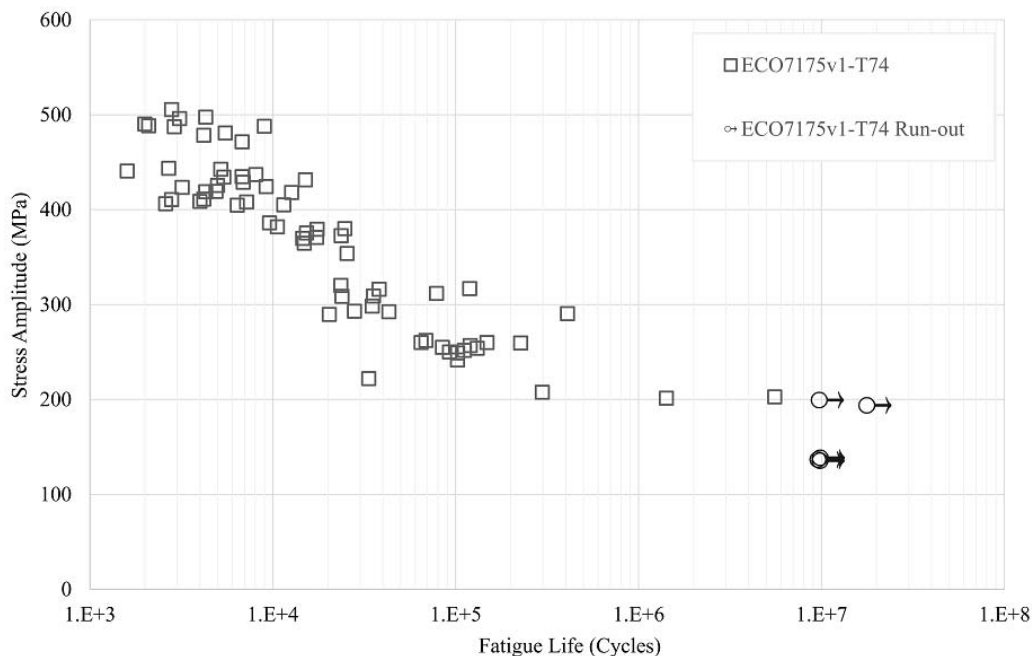


Figure 3: S-N data plot of aluminum ECO7175v1-T74.

1.2 Fracture Analysis

Fatigue fracture surfaces between specimens that were run at higher stresses and those at lower stresses were compared. Specimens subjected to relatively higher stress amplitudes, such as those shown in Figure 4 where the specimens are subjected to 86% UTS, are noted to have relatively more fracture initiation points throughout the outer rim at the surface of the specimens. The fatigue crack propagation bands which originated from these crack initiation points are also relatively short compared to those from specimens subjected to lower stress amplitudes, as in the case of fatigue specimens shown in Figure 5. Fatigue specimens subjected to relatively lower stress amplitudes, such as those in Figure 5, are noted to have relatively fewer crack initiation points. Instead, they typically have longer crack propagation bands that start from these crack initiation points. These crack propagation bands are shown to be capable of reaching halfway or more through the specimens. Fatigue specimens which are subjected to “intermediate” stress amplitudes, such as those specimens subjected between 75% UTS and 55% UTS in Figure 6, have mixed characteristics.

Generally, fatigue crack initiations occur at the surface of the specimens due to slip deformation or surface defects and is the dominant form of fracture initiations. However, crack initiations at the sub-surface are typically found at low stresses and high cycles for high-strength alloys where inclusions are caused by impurities or are part of manufacturing processes such as carburization for case-hardening [11, 13-15]. Conversely, crack initiation sites appear to mainly occur at the surface of the ECO7175v1-T74 specimens rather than the sub-surface, as shown in Figure 7. This may be attributed to the fact the specimens are seemingly free of inclusions. In all cases, the specimens have a relatively uniform and clean surface as there were no clear indications of inclusions or any sort of contaminations from oxides or other intermetallic compound. This is the result of the new composition with the inclusion of calcium which resulted in a cleaner manufacturing process and thus, reduced oxides and other contaminants that are typically introduced into the bulk material due to the reactivity of magnesium. As a result, surface characteristics of the fatigue specimens seem to be the most important aspect of the improved fatigue strength of the ECO7175v1-T74 aluminium alloy.

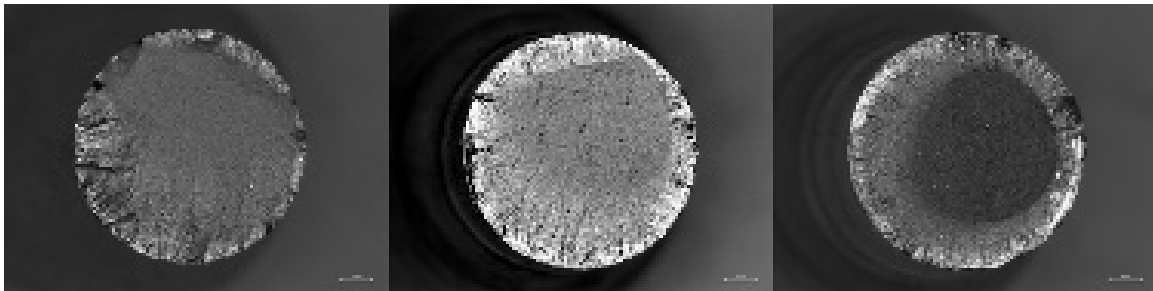


Figure 4: Specimens subjected to 86% UTS. 1 mm scale bar. Specimens at relatively higher stresses have more crack initiation points at the surface compared with specimens at relatively lower stresses. The crack initiation bands that propagate from these crack initiation points are also relatively shorter.

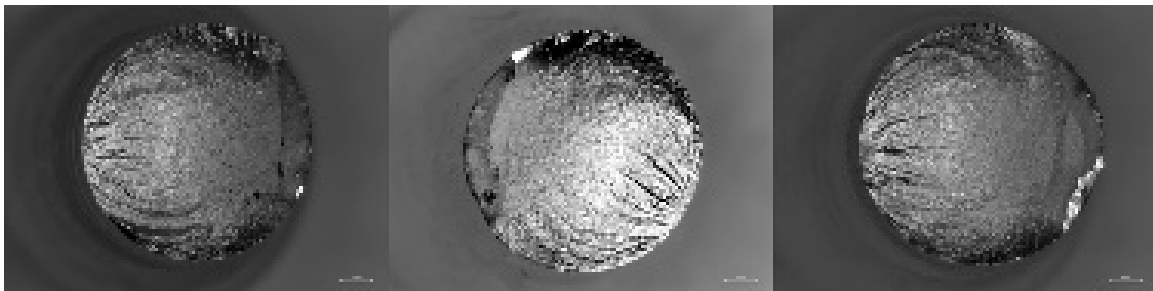


Figure 5: Specimens subjected to 44% UTS. 1 mm scale bar. Specimens at lower stresses typically have fewer crack initiation points but typically have longer crack propagation bands that originate from these crack initiation points.

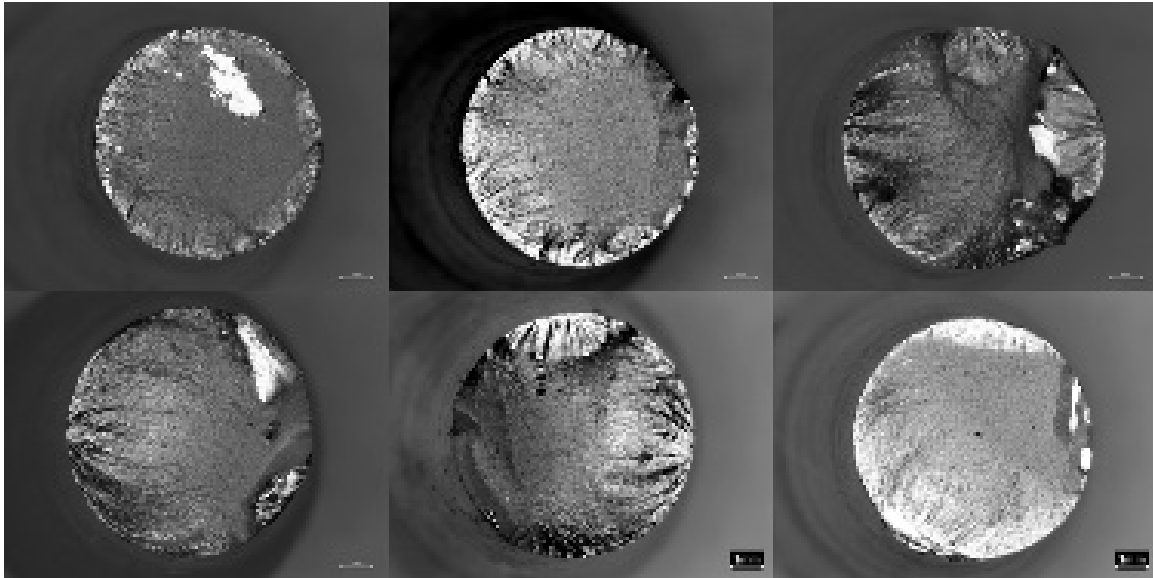


Figure 6: Top three specimens subjected to 75% UTS. Bottom three specimens subjected to 55% UTS. 1 mm scale bar.

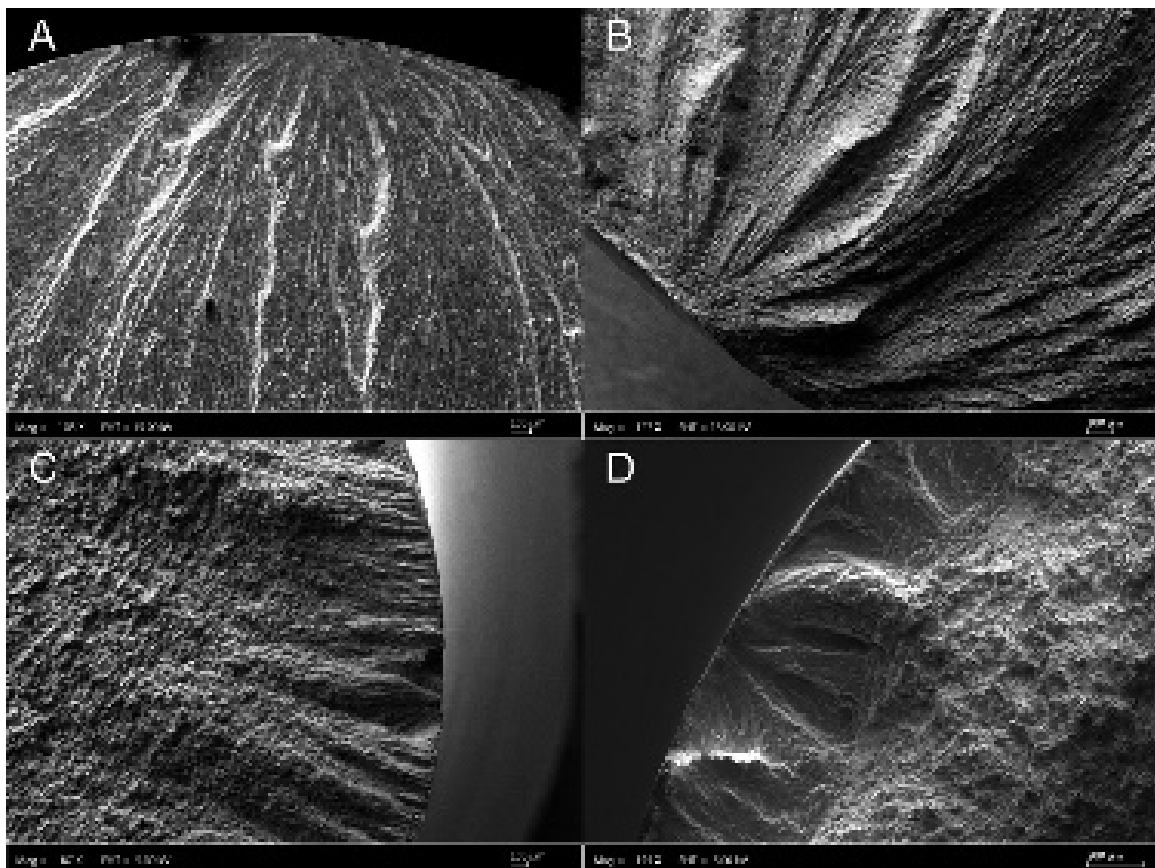


Figure 7: SEM photographs of specimens subjected to (a) 44% UTS; (b) 55% UTS; (c) 75% UTS; and (d) 86% UTS.

4. Conclusion

ECO1775v1 extruded aluminium alloy with temper T74 is subjected to a fully-reversed bending load and examined to find its mechanical characteristics. The generated S-N curve showed that the fatigue life of the new fabricated ECO1775v1-T74 aluminium can exceed 10^7 cycles with a fatigue strength of approximately 207 MPa or less, about

36% of its tensile strength. Fracture analysis indicated that crack surfaces of specimens at high stresses typically exhibited mixed failure modes where the outer rims are predominately ductile and the inner surfaces are predominately brittle. In addition, fracture surfaces of specimens at higher stresses typically have many more crack initiation points around the surface. Conversely, specimens at lower stresses have fewer crack initiation points at the surface of the specimens. Irrespective of stress amplitude, all specimens' crack initiations are seen at the surface and no inclusions to act as stress concentrators were seen at those initiation points.

References

- [1] Aluminum Association. 2015. *International alloy designations and chemical composition limits for wrought aluminum and wrought aluminum alloys*. Arlington, VA: Aluminum Association.
- [2] Battelle Memorial Institute. 2016. *Metallic materials properties development and standardization (MMPDS)*. Columbus, OH: Battelle Memorial Institute.
- [3] Davis, J. R. 1993. *ASM specialty handbook: Aluminum and aluminum alloys*. Materials Park, OH: ASM International.
- [4] Kaufman, G. J. 2000. *Introduction to aluminum alloys and tempers*. Materials Park, OH: ASM International.
- [5] Kim, S. H., K. S. Kim, S. K. Kim, Y. O. Yoon, K. S. Cho, and K. A. Lee. 2012. "Microstructure and mechanical properties of Eco-2024-T3 aluminum alloy." *Adv. Mater. Res.* 602–604: 623–626. <https://doi.org/10.4028/www.scientific.net/AMR.602-604.623>.
- [6] Kim, S. K., and J.-K. Lee. 2011. "Effect of CaO addition on the ignition resistance of Mg-Al alloys." *Mater. Trans.* 52 (7): 1483–1488. <https://doi.org/10.2320/matertrans.M2010397>.
- [7] Kim, S. K., J.-K. Lee, Y.-O. Yoon, and H.-H. Jo. 2006. "Green manufacturing for magnesium alloys." In *Proc., World Foundry Congress*, 1–34. West Midlands, UK: Institute of Cast Metals Engineers.
- [8] Lim, J.-K., S.-J. Hwang, O.-Y. Lee, I.-S. Eun, and D.-S. Shin. 1996. "Fatigue crack growth behavior for 7000 series high strength Al alloys on strengthening heat treatment." In *Proc., 6th Int. Fatigue Conf.*, edited by G. Lütjering and H. Nowack, 947–952. Berlin: Pergamon.
- [9] Lim, S. T., I. S. Eun, and S. W. Nam. 2003. "Control of equilibrium phases (M,T,S) in the modified aluminum alloy 7175." *Mater. Trans.* 44 (1): 181–187. <https://doi.org/10.2320/matertrans.44.181>.
- [10] Lipson, C., and N. J. Sheth. 1973. *Statistical design and analysis of engineering experiments*. New York: McGraw-Hill.
- [11] Mayer, H., W. Haydn, R. Schuller, S. Issler, B. Furtner, and M. Bacher-Höchst. 2009. "Very high cycle fatigue properties of bainitic high carbon–chromium steel." *Int. J. Fatigue* 31 (2): 242–249. <https://doi.org/10.1016/j.ijfatigue.2008.09.001>.
- [12] Nam, T. H., S. H. Kim, J. G. Kim, and S. K. Kim. 2014. "Corrosion resistance of extruded Mg–3Al–1Zn alloy manufactured by adding CaO for the replacement of the protective gases." *Mater. Corros.* 65 (6): 577–581. <https://doi.org/10.1002/maco.201206849>.
- [13] Ochi, Y., T. Matsumura, K. Masaki, and S. Yoshida. 2002. "High-cycle rotating bending fatigue property in very long-life regime of high-strength steels." *Fatigue Fract. Eng. Mater. Struct.* 25 (8–9): 823–830. <https://doi.org/10.1046/j.1460-2695.2002.00575>.
- [14] Shiozawa, K., L. Lu, and S. Ishihara. 2001. "S–N curve characteristics and subsurface crack initiation behaviour in ultra-long life fatigue of a high carbon-chromium bearing steel." *Fatigue Fract. Eng. Mater. Struct.* 24 (12): 781–790. <https://doi.org/10.1046/j.1460-2695.2001.00459>.
- [15] Wang, Q. Y., N. Kawagoishi, and Q. Chen. 2006. "Fatigue and fracture behaviour of structural Al-alloys up to very long life regimes." *Int. J. Fatigue* 28 (11): 1572–1576. <https://doi.org/10.1016/j.ijfatigue.2005.09.017>.